



Seismic Response of 2-D Plane Framed Buildings Eccentrically Braced with Vertical Shear Links

Saher El-Khoriby¹, Ayman Seleemah¹, Ahmed El-Gammal²

¹Professor, Faculty of Engineering, Tanta University, Egypt

E-mail: drsaher2012@yahoo.com

E-mail: seleemah@f-eng.tanta.edu.eg

²Teaching Assistant, Faculty of Engineering, Delta University for Science & Technology, International Coastal Road, Gamasa City, Mansoura, Dakhliya, Egypt

E-mail: ahmedgammal@ymail.com

ABSTRACT

There exist a variety of techniques which can be utilized in seismic-resistant structures in order to protect it from earthquake ground motions. One of these techniques is the employment of vertical eccentrically braced frames (V-EBFs) which dissipate energy during seismic hazard by means of yielding of certain elements, commonly referred to as vertical shear links (VSLs), whereas the whole structures is kept safe in the elastic stage. This paper presents a numerical study on 2-D framed buildings equipped with V-EBFs using two finite element software ANSYS Workbench and ETABS. Each of modal analyses, nonlinear static pushover analyses and nonlinear time history analyses have been conducted on 6 different 2-D framed steel buildings configurations equipped with VSLs made of different metallic alloys, particularly magnesium and steel. Also, how the number of V-EBFs in the building and its placement position influence both the global and local behavior of the buildings have been investigated. Finally, general remarks regarding the optimum conditions of equipping V-EBFs in 2-D framed steel buildings have been pointed out (e.g., VSL material of fabrication, V-EBFs number and placement position).

Keywords: Eccentrically braced frames, vertical shear links, energy dissipation, nonlinear time history analysis, nonlinear static pushover analysis, cyclic loading, seismic loads.

INTRODUCTION

Historical Background

Structures seismic protection systems should satisfy two fundamental criteria. The first is that the structure should have adequate stiffness to keep deflections within the limit of non-structural damage during minor earthquake ground motions, the second is the structures capability to possess enough ductility to avoid collapse in the case of a rare overload which may occur during the major seismic events [1]. One of the efficient seismic protection techniques is to install vertical shear links (VSLs) between chevron braces and the floor beam in certain bays of the buildings thus transforming them into vertical eccentrically braced frames (V-EBFs). V-EBFs serve as the optimal solution to combine the elastic stiffness of concentrically braced frames and the tremendous ductility of moment resisting frames, granting a better response during either frequent or rare seismic events [2]–[10]. In V-EBF system, VSL dissipates the input energy resulting from the earthquake loads through large local inelastic deformations. These inelastic deformations are concentrated in the VSL causing shear yielding. This process guarantees the dissipation of large amount of earthquake input energy, thereby keeping the main structural elements (columns and beams) within the elastic range without any sort of significant damage. After earthquake event

takes place, VSL can be easily replaced since all inelastic deformations are localized in it [1], [11], [12]. Additionally, experimental testing results found in literature proved that inelastic deformation is confined in VSLs, therefore confirming that the VSLs act as ductile fuses to absorb energy [12].

Extensive contributions to the understanding of inelastic deformation of VSLs in V-EBFs resisting seismic loads were mainly carried out during the 1980s [9], [10], [13]–[15]. On the other hand, the seismic response and design methodologies of EBFs have been extensively investigated recently [16]–[20]. Because braces are considered as the lower end support of the VSL, various studies have addressed the topic of braces buckling [20]–[22]. Furthermore, equipping VSLs into the structure is not exclusive to buildings only, but it can be also used in bridges as well. The seismic behavior improvement of bridges with VSLs was investigated previously [23], [24].

In regard to VSL material of fabrication, the most common one is steel. Note that since steel was first utilized as a structural material, many researches were devoted to improve its strength. Anyway, the employment of steel with higher strength in VSLs is not necessarily an advantage since the main function of VSL is to yield rapidly prior to remaining structural members in order to dissipate the maximum possible amount of seismic energy. So, actually the yielding process of VSLs made of steel with higher strength may have a time delay (lag) which would direct earthquake input energy towards the main structural components [25]. Several materials to be used to fabricate VSLs were proposed and investigated (e.g. low strength steel [26], easy going steel [25], aluminum [27]–[30], stainless steel [31], [32], magnesium and copper [32], etc.). Most of these materials were proved to dissipate adequate amount of energy at least under certain circumstances.

Design of Vertical Shear Link

Appropriately designed, VSLs can dissipate earthquake input energy, present high ductility, and retain other structural elements responding elastically. Accordingly, VSL length is an important factor affecting its behavior. Weaker performance of long VSLs in comparison to short ones has been illustrated in numerous investigations [32], [33]. By writing down the equilibrium equation of the VSL assuming that the acting shear forces and bending moments on the link reach $1.5V_p$ and $1.2M_p$, respectively, the VSL length denoted by e can be obtained as follows.

$$e \leq \frac{2 \times 1.2M_p}{1.5V_p} = 1.6 \frac{M_p}{V_p} \quad (1)$$

Where $V_p = \frac{f_{yw}}{\sqrt{3}} t_w (d - t_f)$, and $M_p = f_{yf} b_f t_f (d - t_f)$, are the plastic shear capacity and plastic moment capacity, respectively, for the VSL cross section. Provided that f_{yw} , f_{yf} are the web and flange yield strength, respectively, t_w is the web thickness, d is the overall VSL depth, t_f is the flange thickness, and b_f is the flange width. That formula to determine VSL length was first proposed by Popov and his colleagues [34], [35]. Later on, many researchers proposed novel formulae to determine shorter VSL length in order to meet shear behavior and assure that yielding occurs due to shear force and not bending moments [33], [36]–[38]. However, current codes and standards such as AISC Seismic Provisions (2010) [39] and Eurocode 8 [40] are still adopting Eq. (1).

Another important factor to be considered in the design of VSL is its rotation angle which is limited to 0.08 rad for VSLs having lengths compatible with Eq. 1 [39], [40]. Additionally, existence of stiffeners in VSLs improves its performance via delaying the web buckling and slowing down the load bearing capacity deterioration. For VSLs obeying Eq. (1), stiffener thickness should not be less than the larger of $0.75t_w$ or 10 mm while it should be spaced on distances not exceeding $30t_w - d/5$.

CAPTURING HYSTERETIC BEHAVIOR OF VERTICAL SHEAR LINKS THROUGH FINITE ELEMENT ANALYSES

General

Several finite element software available in market can be employed in order to numerically study full-scale structures eccentrically braced with VSLs (e.g., ANSYS Workbench [41]). However, this software is considered as an all-purpose finite element program providing advanced techniques in the field of finite element analysis in addition to the fact that it is not common to be used by amateur engineers in engineering industry, thus it is often only used by researchers and advanced users. So, modelling of V-EBFs using more common finite element software, such as ETABS [42], has become an urgent need. In order to model those V-EBFs in ETABS, only the hysteretic behavior of VSL is needed as it should be inserted into ETABS. This hysteretic behavior of VSLs can be obtained from either experimental or numerical studies found in literature. In spite of this, and for the sake of completeness, four different VSLs are analyzed in this research using ANSYS Workbench 2020 R1 [41] in order to get their hysteretic behavior. These VSLs are made of two different metallic alloys, typically magnesium and steel. The reason of choosing these two definite alloys is that the 2-D framed building under consideration are expected to have light weight and smaller base shear which makes sense to use VSLs with small yield forces in order to force it to yield quickly before the main structural elements in the building. Thus, using VSLs made of magnesium alloy which has small yield strength meets with the requirements as it enables us also to use VSLs with adequate size cross sections (not tiny ones) thus reducing the effect of web buckling. On the other hand, steel is one of the most common materials in engineering industry and it is convenient to use it to fabricate VSLs.

Three-dimensional Solid Finite Element Modelling

In line with similar previous investigations conducted by the same authors [32], the numerical analyses are performed herein on full-size VSLs. Since the aim of this numerical study is to only get the hysteretic behavior of the VSL, only VSLs are modelled in ANSYS Workbench and there is no need to model the whole V-EBFs; See Reference [32]. The 3-D 20-node solid element SOLID186 [43] is utilized in the meshing of the VSL. The material VSL material of fabrication (magnesium and steel) is modelled with kinematic hardening post-yield behavior. Table 1 illustrates different properties of these alloys. It is worth pointing out that both of these alloys are already included in ANSYS Workbench material library and there is no need to get their specific properties from any external source. The boundary conditions are taken herein following the investigations conducted numerically in [32] in which the bottom face of the VSL is completely fixed while the top face is assigned the cyclic loading protocol. There are numerous cyclic loading protocols available in literature and approved by codes and standards. In this research, a displacement-control cyclic loading protocol, which was previously proposed by Shayanfar et al. [44], is used in the finite element model (Fig. 1). The finite element model of typical VSL is shown in Fig. 2.

Table 1: List of materials properties

Material	Alloy	Young's modulus (MPa)	Tangent modulus (MPa)	Yield strength (MPa)	Ultimate strength (MPa)
Magnesium	ZK61A	45000	920	193	310
Steel	EN 1.0434 +U	200000	1450	250	460

Verification of ANSYS Workbench Finite Element Model

Previous experimental and numerical investigations on VSLs by Hjelmstad and Popov [14] and Baradaran et al. [45] are considered for verification of the finite element modelling process. Specimens 4 and 3 from the studies mentioned above, respectively, are built and analyzed in ANSYS Workbench and their results are compared to the original work. It is obvious in Fig. 3 that the hysteresis loops obtained from ANSYS Workbench almost agree with the ones provided in literature from the point of energy dissipation capacities and ultimate strengths. Moreover, it is evident that modelling of the VSL only is sufficient to capture its hysteretic behavior and there is no need to model the whole frame.

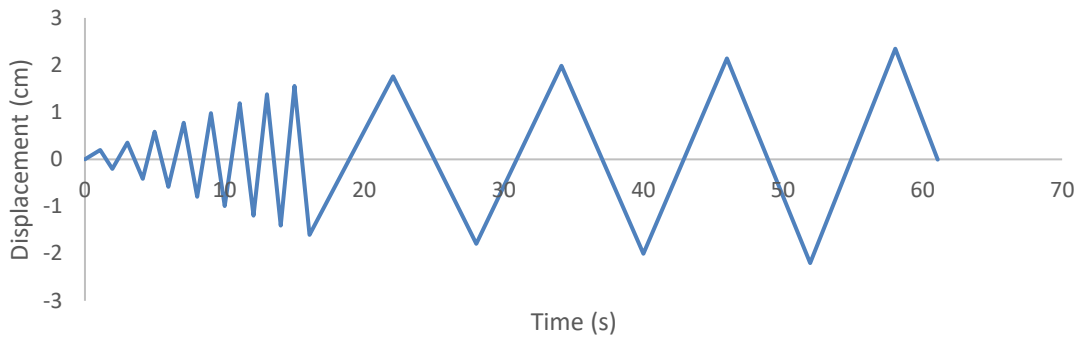


Fig. 1: Displacement-control cyclic loading protocol applied to VSL [44]



Fig. 2: Finite element model of typical VSL

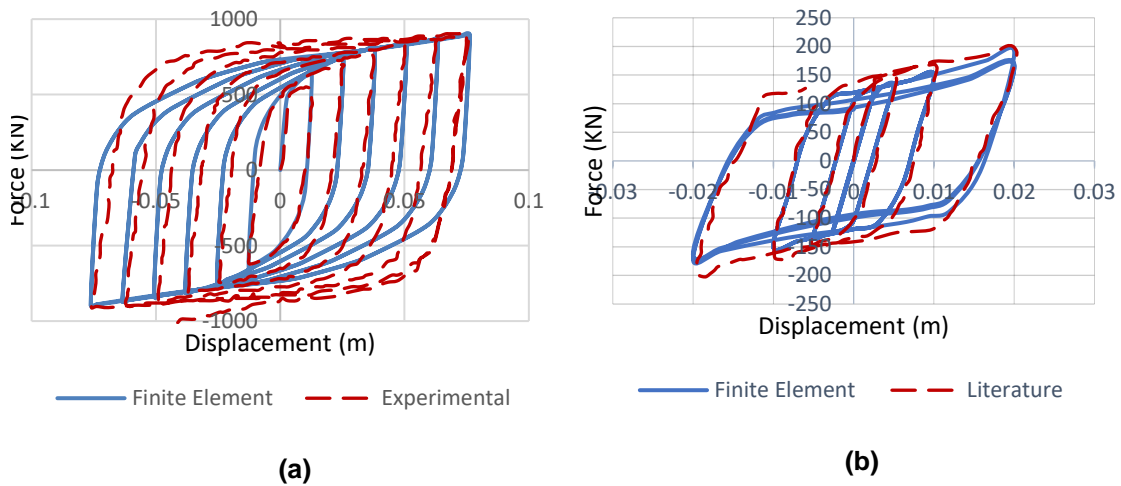


Fig. 3: Verification study hysteresis loops, (a) Hjelmsstad and Popov [14], (b) Baradaran et al. [45]

Description of the Specimens

In order to design VSLs (i.e., get their number of stiffeners and their thickness, and the spacing between them), a MATLAB code [46] based on AISC and Eurocode requirements (previously

written by the same authors [32]) is used. However, adopting the same equations would result in VSLs with very small dimensions which are not easily applicable in practice. Thus, VSLs dimensions are somehow increased in order to get more adequate specimens. Although AISC seismic provisions code and Eurocode 8 are only concerned with steel V-EBFs and there are no specific formulae to design VSLs fabricated from magnesium available in literature, magnesium VSLs are designed through the same methodology of designing steel ones. Table 2 summarizes the design parameters of VSLs specimens.

Table 2: Summary of specimens' design parameters

Specimen	Material	Dimensions (mm)*	e (mm)	Stiffeners	
				Thickness (mm)	Spacing (mm)
1	Magnesium	20-3-34-3	300	10	100
2	Magnesium	30-3.8-44-3.5	300	10	100
3	Steel	28-3-51.2-3.4	300	10	100
4	Steel	46-5.2-69.6-3.8	300	10	100

*flange width-flange thickness-web clear depth-web thickness

Analyses Results

The hysteresis loops obtained from the 3-D finite element analyses are shown in Fig. 4. As observed, all specimens exhibited stable and fat hysteresis loops without any sort of stiffness degradation and it is evident that steel VSLs have much higher initial stiffness compared to magnesium ones. Since the amount of dissipated energy is the primary key parameter to assess the efficiency of VSL, the cumulative dissipated energy per each cycle is comparatively given in Fig. 5 for all four specimens. It is worth pointing out that the amount of dissipated energy is determined by calculating the area of the hysteresis loop in each cycle using the data analysis software OriginPro 2019 [47]. It is obvious that specimen 4 dissipates the maximum possible amount of energy under the applied loading conditions. Fig. 6 shows a plot of equivalent von-Mises stress for each specimen and it can be observed that all of the specimens successfully survived the applied cyclic loading conditions without failure since the maximum equivalent von-Mises stress is lower than the ultimate strength of the material. It is also noticeable that the maximum angle of rotation of all of the specimens is equal to 0.079 rad. which is within the allowable limit of 0.08 rad according to AISC Seismic Provisions and Eurocode 8. In order for the hysteretic behavior of VSLs to be extracted and then inserted back into ETABS, three main properties are required, particularly VSL yield force, initial stiffness and post-yield stiffness ratio with respect to the initial stiffness. All of these properties can be found by plotting the envelope of the hysteresis loop for each specimen as shown in Fig. 7. Table 3 indicates the extracted data from the envelope of the hysteresis loops which are required to be inserted into ETABS.

Table 3: VSLs properties to be inserted into ETABS

Specimen	Yield shear force (KN)	Initial stiffness (KN/m)	Post-yield stiffness ratio
1	4.32	900	0.125
2	10.24	2898	0.148
3	12.82	11978	0.073
4	30.4	37998	0.026

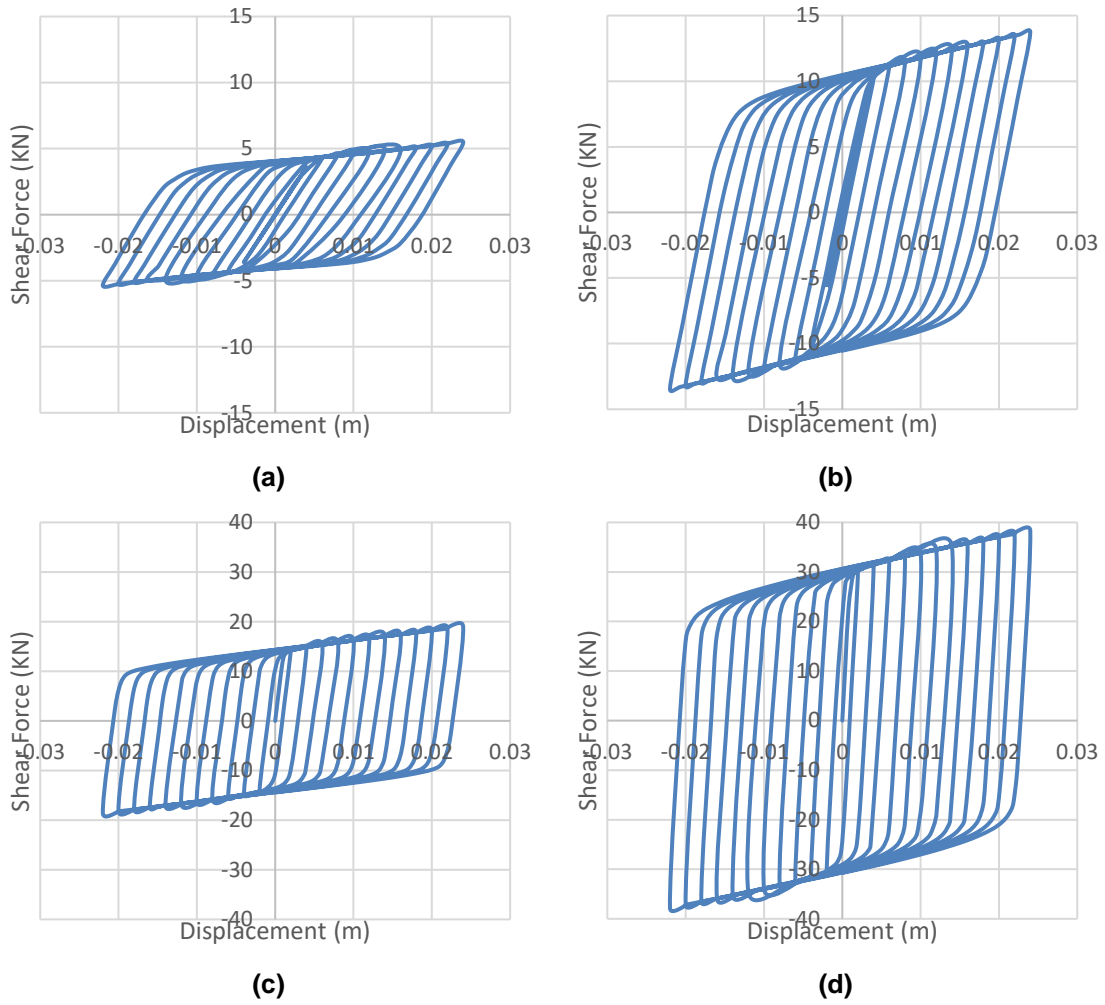


Fig. 4: Hysteresis loops of the specimens, (a) specimen 1, (b) specimen 2, (c) specimen 3, (d) specimen 4

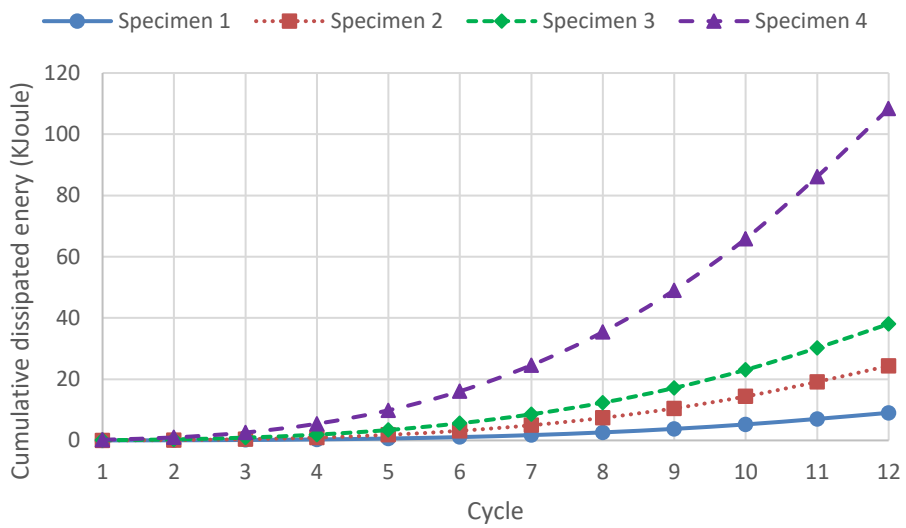


Fig. 5: Cumulative dissipated energy per each cycle

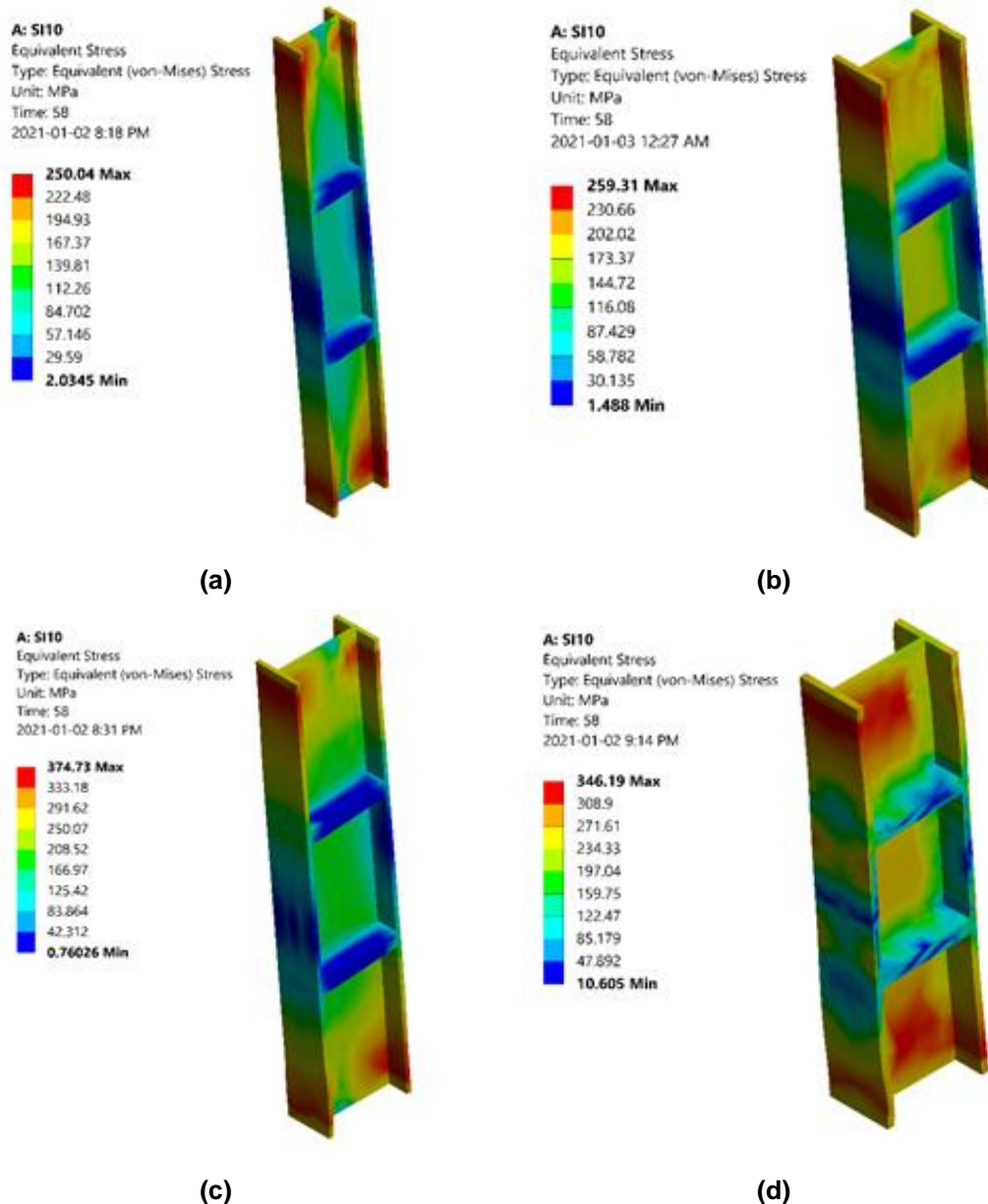


Fig. 6: Equivalent von-Mises stress of the specimens, (a) specimen 1, (b) specimen 2, (c) specimen 3, (d) specimen 4

DESCRIPTION OF THE 2-D FRAMED BUILDINGS

The building to be studied is a 10-storey 2-D steel plane framed building consisting of 3 bays each of 5 m span. The bottom story height is 4.5 m whilst the typical story height is 3m. All the beams and columns are fabricated from ASTM A572 Gr. 50 steel which has a yield strength of 345 MPa and an ultimate strength of 450 MPa. HLS260 sections are adopted for main structural elements in the building. Some bays of the original building are equipped with the VSLs analyzed above in order to transform them into V-EBFs thus improving the seismic response of the building. The chevron braces to be equipped in the V-EBFs have a cross section of Pipe12XS and it is made from the same steel grade of the beams and the columns. Five different configurations of the building are proposed and summarized in Table 4.

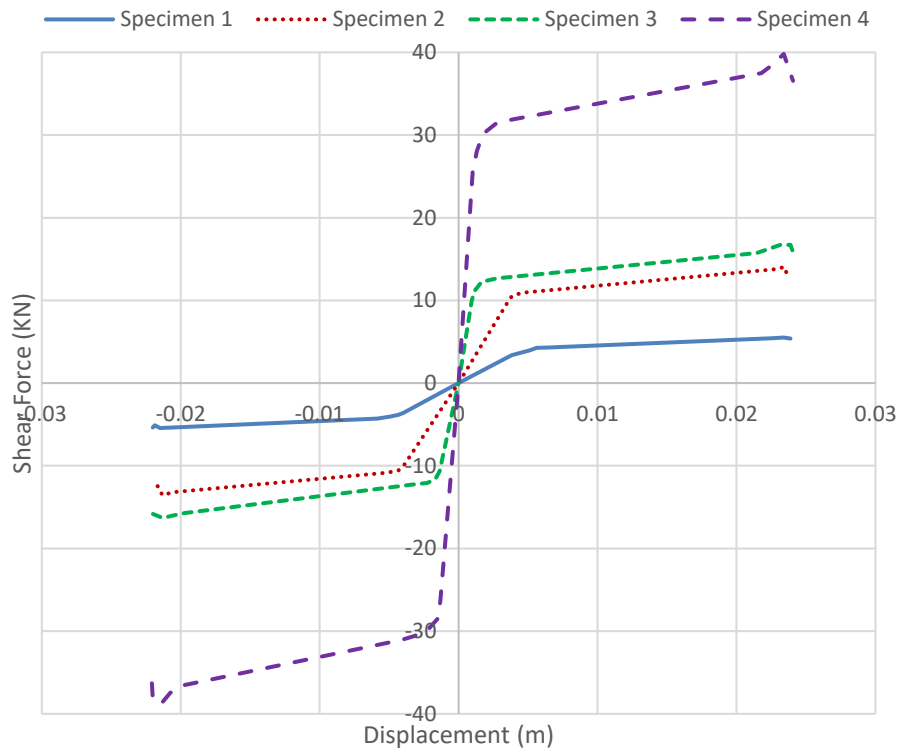


Fig. 7: Envelope of the hysteresis loops for each specimen

Table 3: VSLs locations in the building

Building configuration	Story			
	1	2	3	4 to 10
B1	----	----	----	----
B2	Specimen 1	----	----	----
B3	Specimen 1	Specimen 1	Specimen 1	----
B4	Specimen 2	----	----	----
B5	Specimen 3	----	----	----
B6	Specimen 4	----	----	----

FINITE ELEMENT MODELLING OF THE BUILDING

General

Modal analyses, nonlinear static pushover analyses and nonlinear time history analyses are performed on all buildings configurations for the sake of assessing their seismic response. Thereupon, nonlinear 3-D models of the six buildings configurations are built and analyzed using the finite element computer program ETABS 18.1.1 [42]. Regarding beams, columns and chevron braces, they are all modelled utilizing 3-D frame elements which have six degrees of freedom at each node. The nonlinear response of these frame elements is modelled by defining plastic hinges either at the ends of the beams and columns, or at the middle of each brace. Hinges properties are automatically calculated by ETABS according to ASCE 41-17 [48]. In order to simulate the buildings response when equipped with V-EBFs, VSLs should be defined in its desired location as plastic Wen link element [49]–[51] based on the hysteretic response previously extracted from ANSYS Workbench in Table 3. The foundations of the buildings are assumed to be totally restrained disregarding the effect of soil-structure interaction.

Verification of ETABS Finite Element Model

At the beginning, ETABS finite model should be verified in order to justify its capability of simulating the response of V-EBFs equipped with VSLs depending on the data extracted from the hysteresis loops. The specimen selected for the current verification study is the same one tested by Baradaran et al. [45] (specimen 3) which was previously verified in this paper using ANSYS Workbench. ETABS finite element model consists of a single-story single-span V-EBF modelled as the same manner provided above. V-EBF is made of steel with yield and ultimate stresses of 350 and 500 MPa and consisting of beam, columns and bracing with cross-sections of IPB140, IPB120 and 2UNP100, respectively. VSL properties are extracted from the hysteresis loops provided in the same paper by Baradaran and his colleagues based on experimental and numerical tests and then inserted back into plastic Wen link element properties in ETABS. A force-control cyclic loading protocol is then applied to the V-EBF beam (it is noticeable that ETABS 18.1.1 does not provide any straightforward technique to apply displacement-control cyclic loading protocol to a portion of the structure rather than its base). Fig. 8 illustrates the efficiency and accuracy of ETABS finite element model as the base shear-displacement curve obtained from ETABS is consistent with the curve provided by Baradaran et al. along with some tiny differences. Though these differences are still within the accepted range. Subsequently, it is reliable to correctly simulate the response of V-EBFs equipped with VSLs using ETABS based on the input VSLs hysteretic data.

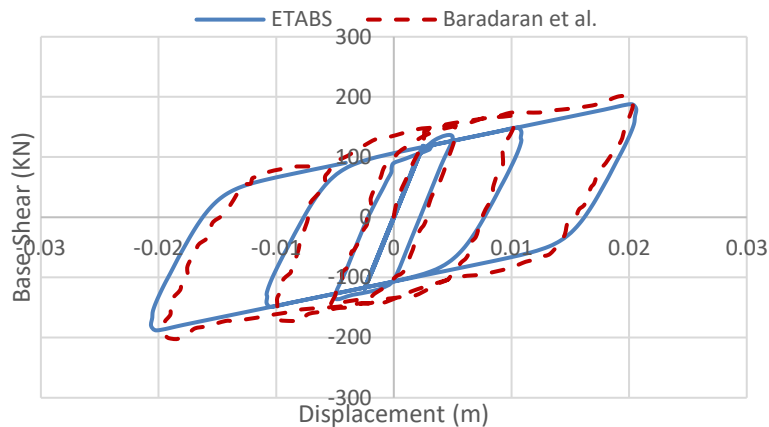


Fig. 8: Results obtained from ETABS vs. results provided by Baradaran et al. [45]

RESULTS AND DISCUSSION

Modal Analyses

Since the first mode shape is the dominant in most basic structures, modal analyses are conducted on the proposed buildings in order to evaluate the effect of installing VSLs on the first mode shape and its time period. Fig. 9 demonstrate the first mode shape of all of the six buildings accompanied with its corresponding time period. It can be easily detected that installing VSLs in the building increased its stiffness, however, stiffness of a system is inversely proportional to its time period and this interpret the current situation as all buildings configurations equipped with VSLs (B2 to B6) have lower time periods than the original bare one (B1). Yet, the decrease of the time period of buildings (B2 to B6) ranges from 3% to 16% and this is not considered a significant change especially in the case of small time period values as the current case.

Nonlinear Static Pushover Analyses

The response of the buildings in its different configurations is evaluated based on the results of the nonlinear static pushover analyses. Fig. 10 shows a plot of base shear vs. top roof displacement of all buildings. As noticed, all buildings containing VSLs (B2 to B6) have higher elastic lateral stiffness compared to the original bare building (B1). This emphasizes the modal

analyses results presented earlier, particularly the timer period results. It is also clear that configurations B5 and B6 (containing steel VSLs) has much higher ductility compared to the other configurations whilst configuration B2 (containing single magnesium VSL) has a nearly identical response to that of B3 (containing three magnesium VSLs) so there is no significant benefit of increasing the number of VSLs in the building in that particular case. Concerning buildings attitude under the effect of lateral loads, it is assessed counting on determining the performance level at the performance point which is generally measured in terms of member rotations as per FEMA 356 [52]. Although the performance level of the original bare building B1 lies in the life safety (LS) level, installation of VSLs in the other buildings configurations managed to shift their performance towards the operational-immediate occupancy (IO) region, therefore, having less drift, and upgraded performance (i.e., lower non-structural damage) (Table 4). Despite specimen 4 of the preliminary study on ANSYS Workbench exhibited the highest amount of dissipated energy under the effect of cyclic loading and as a result one may conclude that it is the best specimen to be installed in the building to improve its seismic resistance, this is proved to not being true under the effect of lateral load in nonlinear static pushover analyses since the performance level of the building equipped with specimen 4 (B6) lies in the immediate occupancy (IO) level while certain buildings configurations equipped with weaker VSLs specimens managed to retain the building in the operational performance level. Thus, the response of VSLs subjected to cyclic loading is not always sufficient to determine its efficiency when equipped to full-scale building subjected to real earthquake loadings.

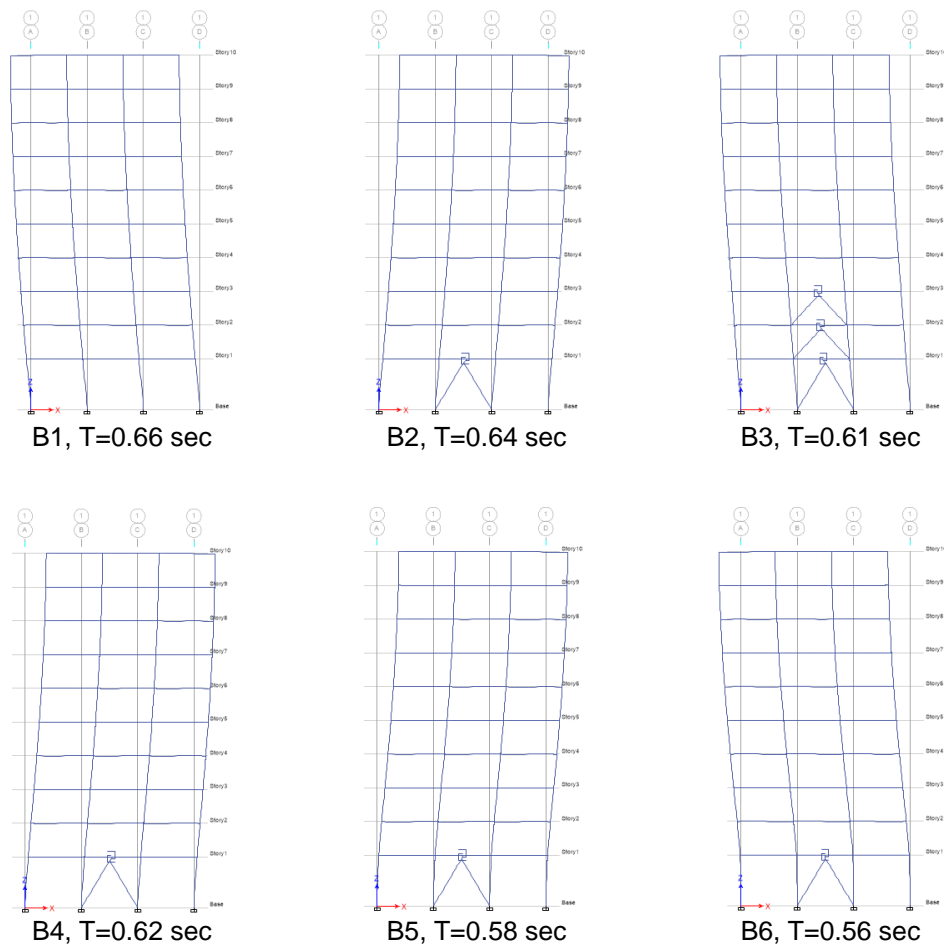


Fig. 9: First mode shapes of the buildings along with tis corresponding time period

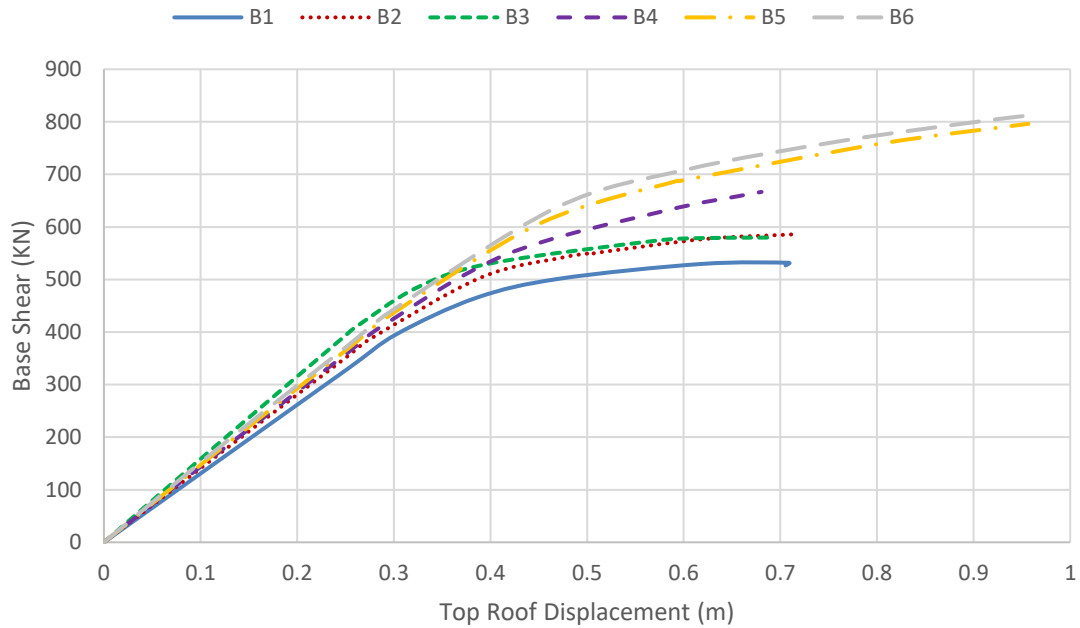


Fig. 10: Pushover curves of the buildings

Table 4: Details of hinges for the buildings

Building configuration	A-B	B-IO	IO-LS	LS-CP	Beyond CP	Performance level
B1	132	4	4	0	0	LS
B2	139	3	0	0	0	IO
B3	146	0	0	0	0	Operational
B4	141	1	0	0	0	IO
B5	142	0	0	0	0	Operational
B6	141	1	0	0	0	IO

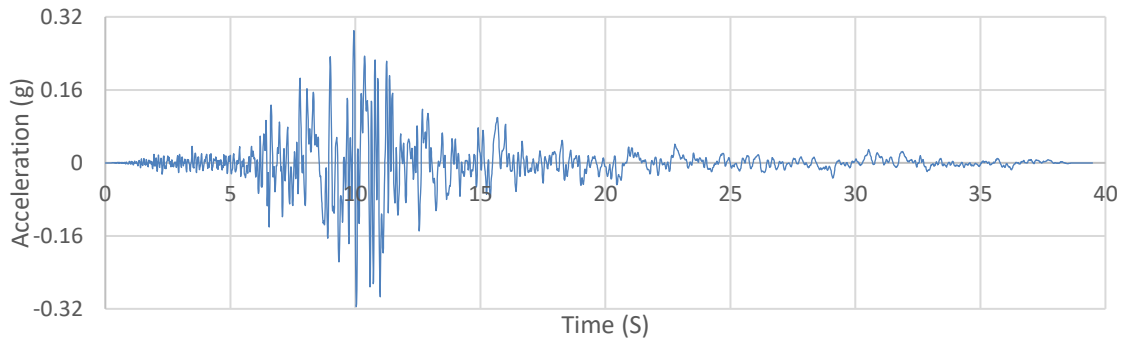
Nonlinear Time History Analyses

In order to study the buildings response under real earthquake histories, Imperial Valley (USA) earthquake October 15, 1979 is chosen to be assigned to the buildings for the nonlinear time history analyses. This particular earthquake has a peak ground acceleration of nearly 0.32g and a frequency range of 0.1 to 40 Hz. Source of earthquake history and data is PEER (Pacific Earthquake Engineering Research) Strong Motion Database based on USGS STATION 5115 recording station. Fig. 11 presents the time history of the earthquake and its response spectrum.

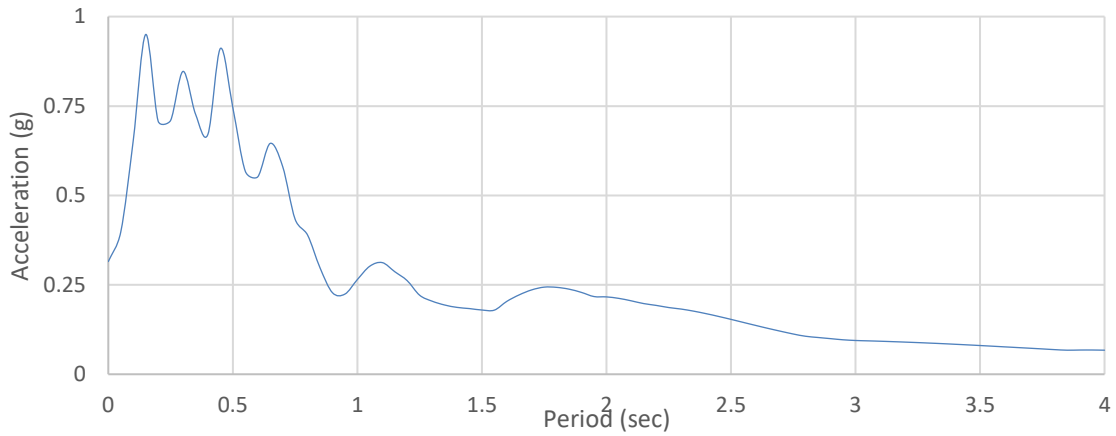
Referring to Fig. 12, it is seen that the maximum base shear acting on the building during the earthquake is greatly affected by the installation of VSLs. Generally speaking, increasing the stiffness of the building by VSLs should induce larger base shears. Yet, this is not always applicable since the applied earthquake has a response spectrum containing several ups and downs (not smooth envelope one), this intercepts the case under study in which, for instance, B6 has lower base shear compared to B5 in spite of having slightly more stiffness as shown previously in Fig. 10.

As appearing in Fig. 13(a), installation of VSLs into the building did not much change the whole building deformed shape, however, it resulted into decreasing the maximum story displacements in comparison with the original bare building (B1). Since configurations B3 and B5 were proved to be lying in the operational performance level, more attention should be directed towards them as they are more favorable to be employed in the building under consideration. These

configurations have maximum story displacements of 79% and 64%, respectively, of that of the original bare building (B1). The advantage of B5 on B3 is due to the fact that it exhibits more stiffness as revealed above in Fig. 10, hence B3 has relatively lower story displacements.



(a)



(b)

Fig. 11: Imperial Valley 1979 Earthquake, (a) time history, (b) response spectrum

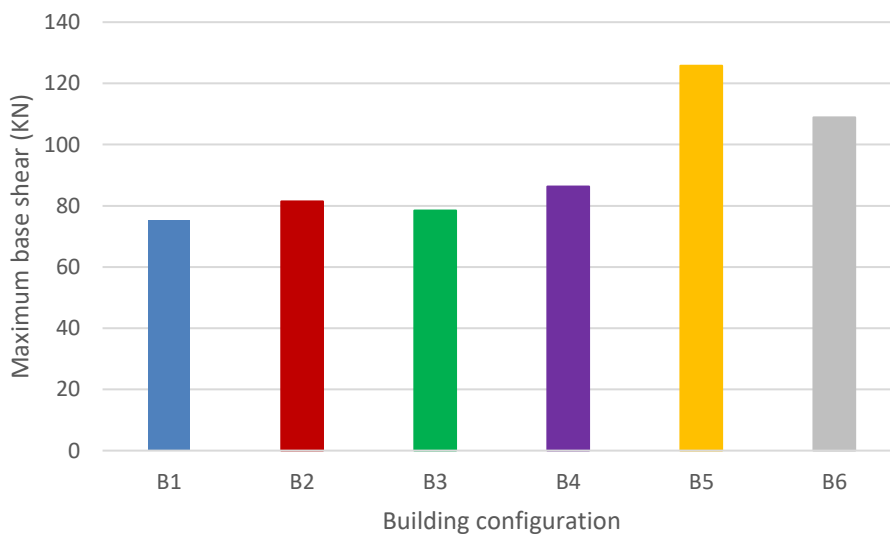


Fig. 12: Maximum base shear of the buildings

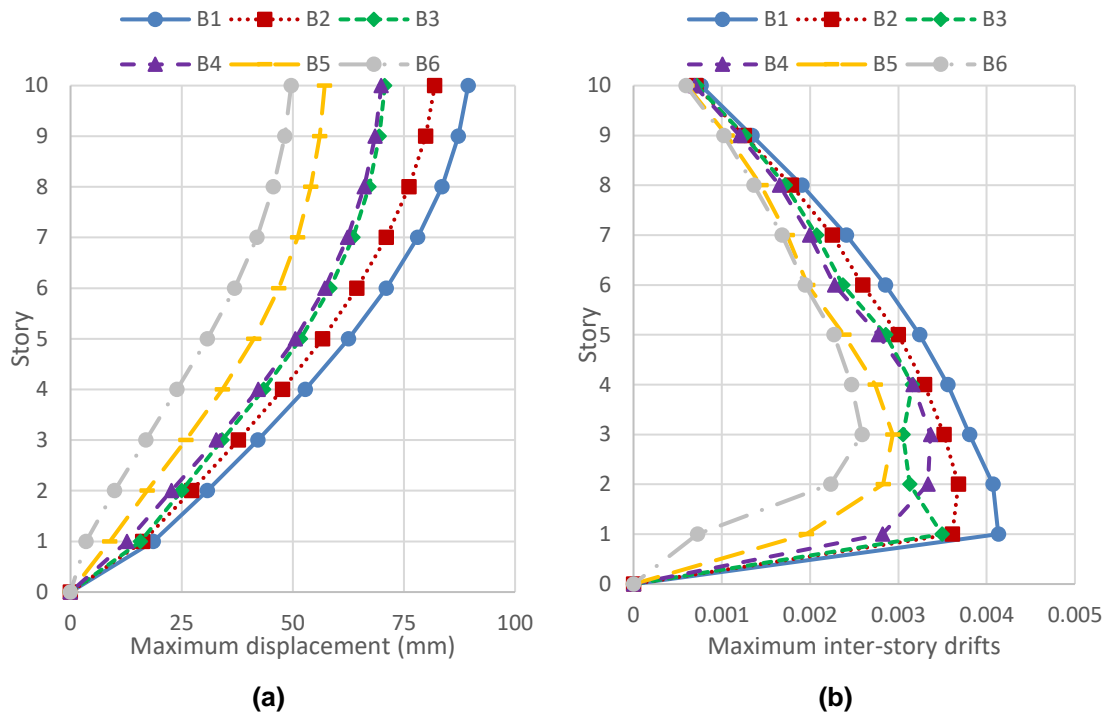


Fig. 13: Global response of the buildings, (a) maximum story displacements, (b) maximum inter-story drifts

With respect to the maximum inter-story drifts of the buildings during the applied earthquake (Fig. 13(b)), it is found that the buildings installed with VSLs have lower inter-story drifts compared to the one without VSLs (B1). Putting the light on the more favorable configurations (B3 and B5), it is obvious that they have maximum inter-story drifts of 0.35 and 0.29, respectively, which in turn represent about 85% and 71% of the maximum inter-story drift of the original building (B1), respectively. Taking into account the local deformation of the building, B3 is able to modify the buildings local inter-story drifts (especially up to the fourth story) and this is due to the existence of VSLs near that particular portion of the building. Fig. 14 compares the hysteresis loops of the VSLs of different configurations but herein obtained from ETABS. It can be simply recognized that these hysteresis loops, generated based on the data extracted from ANSYS Workbench, are compatible with those attained from the previously mentioned software.

As previously reported in literature, the main role of the VSLs in the building is to dissipate energy by yielding whereas the main structural elements are kept safe responding elastically. Thus, the ratio of the dissipated hysteretic energy (EH) to the earthquake input energy (EI) is shown in Fig. 15. Note that B1 does not include any mechanism to dissipate hysteretic energy. It is visible that the configuration B5 (containing VSL specimen 3) is the one capable of dissipating the greatest amount of energy among all other configurations although specimen 3 was one step behind specimen 4 in terms of dissipating energy when subjected to cyclic loading. This supports the rule that dissipating large amount of energy under cyclic loading conditions does not necessary mean that the VSL is capable to dissipate the same amount of energy during earthquake event. The reason is that VSLs exposed to cyclic loading are forced to displace in certain directions with definite displacements and this is not the case when earthquake takes place since stories displacements are mainly dependent on the characteristics of the building and the lateral load resisting system (e.g., stiffness, time period, etc.). Another factor to be considered is the time delay of the VSL which can be defined as the time required for the VSL to yield and start to dissipate energy exhibiting hysteretic behaviour. As shown in Fig. 15, configuration B5 again has the lowest time delay of 2.95 sec so it is predicted to yield quickly compared to other proposed configurations.

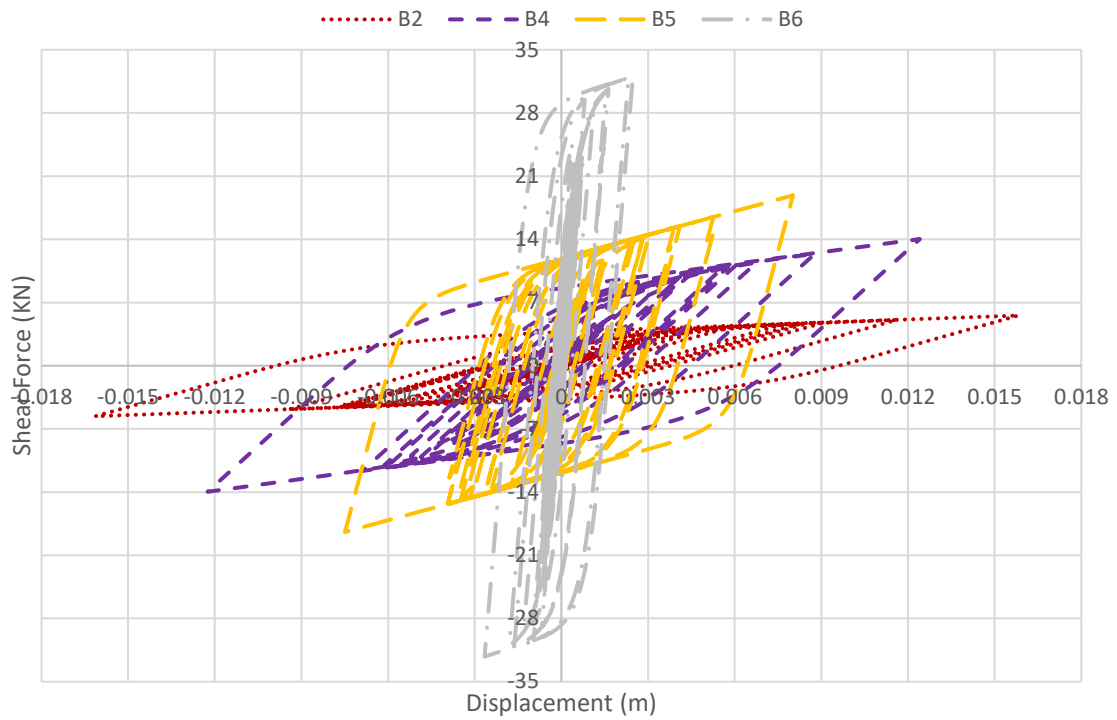


Fig. 14: Hysteresis loops of single VSLs

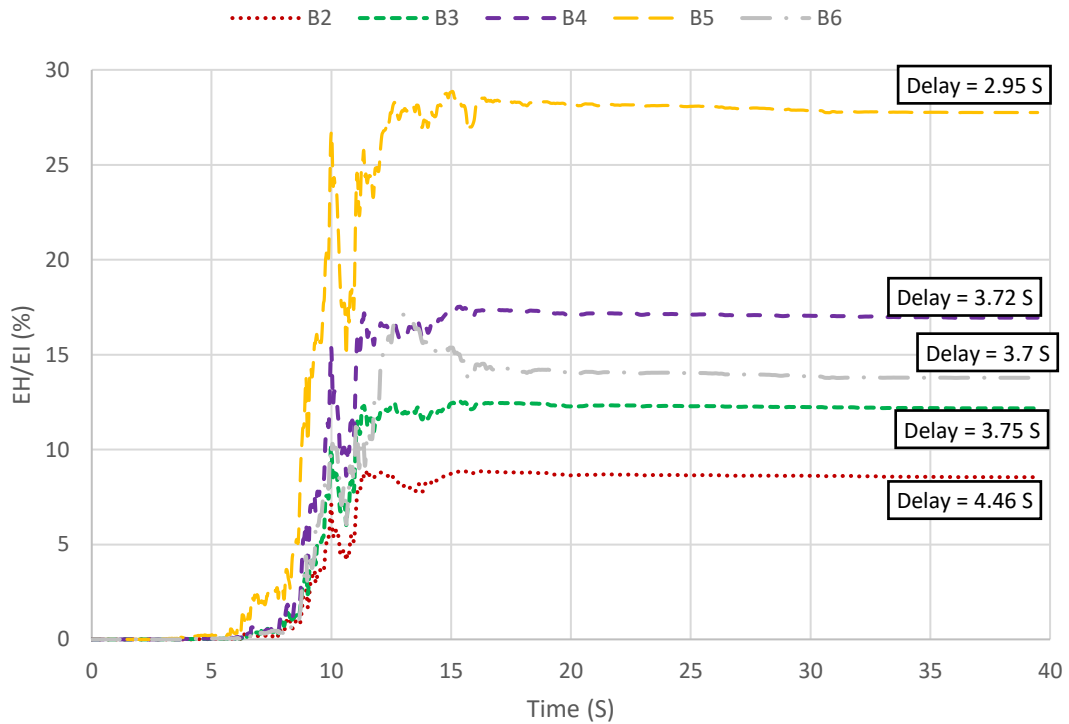


Fig. 15: Ratio of dissipated hysteretic energy to earthquake input energy during seismic event

CONCLUSIONS

A numerical investigation is conducted on a three-bays ten-story 2-D steel plane framed building, using the finite element software ETABS, in order to evaluate its seismic response in its original bare condition and in the case of equipping it with VSLs in certain bays of it transforming them into V-EBFs. In order for the VSLs to be defined in ETABS, their hysteretic behavior should be first captured and certain parameters should be determined (e.g., VSL yield force, initial stiffness and post-yield stiffness ratio). Though hysteretic behavior of VSLs may be found in literature, a number of 4 VSLs specimens have been proposed and their hysteretic behavior has been captured using the finite element software ANSYS Workbench. This hysteretic behavior has been inserted back into ETABS yielding 6 different buildings configurations. The response of these configurations is assessed and compared utilizing modal analyses, nonlinear static pushover analyses and nonlinear time history analyses.

- 1- VSLs can be modelled efficiently in ANSYS Workbench without any significant need to model the whole V-EBFs if it is only desired to capture its hysteretic behavior under cyclic loading.
- 2- The amount of dissipated energy is directly proportion to the VSL lateral stiffness when it is subjected to cyclic loading. Moreover, the bulkier VSLs exhibited more shear yielding behavior therefore having a great chance to yield in shear rather than flexure.
- 3- Adopting the conventional equations to design VSLs exposed to low shear forces would lead to very small dimensions which are not easily applicable in practice, thus it is recommended to slightly increase VSLs attained dimensions. However, this issue needs be furtherly investigated.
- 4- Hysteretic behavior of VSLs obtained from experimental or numerical investigations can be inserted back into ETABS via Wen link element in order to simulate VSLs response in full-scale buildings.
- 5- Modal analyses results revealed that installation of VSLs in the building resulted in a change in its stiffness and thus a change in its first mode time period. However, that change is not significant in that particular case of study.
- 6- Nonlinear static pushover analyses results indicated that despite the original building lies in the life safety performance level, the buildings configurations including VSLs lies within the operational to immediate occupancy performance levels. It is also found that buildings equipped with steel VSLs exhibit more ductility and lateral stiffness compared to those equipped with magnesium ones.
- 7- Nonlinear time history analyses results showed that the buildings installed with VSLs have lower story displacements and inter-story drifts in comparison with the original bare building. Additionally, it was found that the building configuration B5, in which VSL specimen 3 is employed in the first story only, has the maximum amount of dissipated hysteretic energy compared to other configurations although specimen 3 was not the one dissipating maximum amount of energy when subjected to cyclic loading. Moreover, configuration B5 began to dissipate energy quickly and before other configurations thus the VSL in this configuration would not need much time to begin operating. Thereupon, it is obvious that this configuration managed to improve the overall building performance keeping it within the operational performance level and it is proved to be more favourable and advantageous over other configurations in terms of story displacements, inter-story drifts, hysteretic energy dissipation and time delay.
- 8- A VSL dissipating large amount of energy under cyclic loading conditions does not necessary mean that the same VSL is capable to dissipate the same amount of energy during earthquake event. The reason is that VSLs exposed to cyclic loading are forced to displace in certain directions with definite displacements and this is not the case when earthquake takes place since stories displacements are mainly dependent on the characteristics of the building and the lateral load resisting system (e.g., stiffness, time period, etc.).

REFERENCES

- [1] M. Bulic and M. Causevic, "Numerical investigation of short seismic links in shear," *Ce/Papers*, vol. 1, no. 2–3, pp. 3249–3258, 2017, doi: 10.1002/cepa.378.
- [2] M. D. Engelhardt and E. P. Popov, "On design of eccentrically braced frames," *Earthq. spectra*, vol. 5, no. 3, pp. 495–511, 1989.
- [3] K. D. Hjelmstad and Sang-Gab Lee, "Lateral buckling of beams in eccentrically-braced frames," *J. Constr. Steel Res.*, vol. 14, no. 4, pp. 251–272, 1989, doi: 10.1016/0143-974X(89)90039-4.
- [4] E. P. Popov, "Recent research on eccentrically braced frames," *Eng. Struct.*, vol. 5, no. 1, pp. 3–9, 1983.
- [5] Y. Qi, W. Li, and N. Feng, "Seismic collapse probability of eccentrically braced steel frames," *Steel Compos. Struct.*, vol. 24, no. 1, pp. 37–52, 2017, doi: 10.12989/scs.2017.24.1.037.
- [6] R. K. Mohammadi and A. H. Sharghi, "On the optimum performance-based design of eccentrically braced frames," *Steel Compos. Struct.*, vol. 16, no. 4, pp. 357–374, 2014.
- [7] M. Lian, M. Su, and Y. Guo, "Seismic performance of eccentrically braced frames with high strength steel combination," *Steel Compos. Struct.*, vol. 18, no. 6, pp. 1517–1539, 2015.
- [8] P. W. Richards and C.-M. Uang, "Effect of flange width-thickness ratio on eccentrically braced frames link cyclic rotation capacity," *J. Struct. Eng.*, vol. 131, no. 10, pp. 1546–1552, 2005.
- [9] K. Kasai and E. P. Popov, "Cyclic web buckling control for shear link beams," *J. Struct. Eng.*, vol. 112, no. 3, pp. 505–523, 1986.
- [10] C. W. Roeder and E. P. Popov, "Eccentrically braced steel frames for earthquakes," *J. Struct. Div.*, vol. 104, no. 3, pp. 391–412, 1978.
- [11] S. Caprili, F. Morelli, N. Mussini, and W. SALVATORE, "Experimental tests on real-scale EBF structures with horizontal and vertical links," *Data Br.*, vol. 21, no. October, pp. 1246–1257, 2018, doi: 10.1016/j.dib.2018.10.126.
- [12] M. G. Vetr, A. Ghamari, and J. Bouwkamp, "Investigating the nonlinear behavior of Eccentrically Braced Frame with vertical shear links (V-EBF)," *J. Build. Eng.*, vol. 10, no. February, pp. 47–59, 2017, doi: 10.1016/j.jobe.2017.02.002.
- [13] K. D. Hjelmstad and E. P. Popov, "Seismic Behavior of Active Links in Eccentrically Braced Frame," Report No. UCB/EERC, 1983.
- [14] K. D. Hjelmstad and E. P. Popov, "Cyclic behavior and design of link beams," *J. Struct. Eng.*, vol. 109, no. 10, pp. 2387–2403, 1983.
- [15] K. D. Hjelmstad and E. P. Popov, "Characteristics of Eccentrically Braced Frames," *J. Struct. Eng.*, vol. 110, no. 2, pp. 340–353, Feb. 1984, doi: 10.1061/(asce)0733-9445(1984)110:2(340).
- [16] D. Dubina, A. Stratan, and F. Dinu, "Dual high-strength steel eccentrically braced frames with removable links," *Earthq. Eng. Struct. Dyn.*, vol. 37, no. 15, pp. 1703–1720, Dec. 2008, doi: 10.1002/eqe.828.
- [17] M. Bosco and P. P. Rossi, "Seismic behaviour of eccentrically braced frames," *Eng. Struct.*, vol. 31, no. 3, pp. 664–674, 2009, doi: 10.1016/j.engstruct.2008.11.002.
- [18] L. Mastrandrea and V. Piluso, "Plastic design of eccentrically braced frames, I: Moment-shear interaction," *Journal of Constructional Steel Research*, vol. 65, no. 5, pp. 1007–1014, 2009, doi: 10.1016/j.jcsr.2008.10.002.
- [19] K. C. Lin, C. C. J. Lin, J. Y. Chen, and H. Y. Chang, "Seismic reliability of steel framed buildings," *Struct. Saf.*, vol. 32, no. 3, pp. 174–182, 2010, doi: 10.1016/j.strusafe.2009.11.001.
- [20] R. Montuori, E. Nistri, and V. Piluso, "Theory of plastic mechanism control for eccentrically braced frames with inverted y-scheme," *J. Constr. Steel Res.*, vol. 92, pp. 122–135, 2014, doi: 10.1016/j.jcsr.2013.10.009.
- [21] A. A. Karalis and K. C. Stylianidis, "Experimental investigation of existing R/C frames strengthened by high dissipation steel link elements," *Earthq. Struct.*, vol. 5, no. 2, pp. 143–160, 2013, doi: 10.12989/eas.2013.5.2.143.
- [22] R. Montuori, E. Nistri, and V. Piluso, "Rigid-plastic analysis and moment-shear interaction for hierarchy criteria of inverted y EB-Frames," *J. Constr. Steel Res.*, vol. 95, pp. 71–80, 2014, doi: 10.1016/j.jcsr.2013.11.013.
- [23] J. W. Berman and M. Bruneau, "Supplemental system retrofit considerations for braced

- steel bridge piers," *Earthq. Eng. Struct. Dyn.*, vol. 34, no. 4–5, pp. 497–517, 2005, doi: 10.1002/eqe.448.
- [24] J. W. Berman and M. Bruneau, "Approaches for the seismic retrofit of braced steel bridge piers and proof-of-concept testing of an eccentrically braced frame with tubular link," Citeseer, 2005.
- [25] A. S. Daryan, H. Bahrampoor, M. Ziaei, A. Golafshar, and M. A. Assareh, "Seismic behavior of vertical shear links made of easy-going steel," *Am. J. Eng. Appl. Sci.*, vol. 1, no. 4, 2008.
- [26] Y. Shinabe and Y. Takahashi, "The present state of eccentric brace design in Japan," in *Proceedings of the 4th Pacific Structural Steel Conference, Singapore*, 1995, pp. 813–820.
- [27] D. C. Rai and B. J. Wallace, "Aluminium shear-links for enhanced seismic resistance," *Earthq. Eng. Struct. Dyn.*, vol. 27, no. 4, pp. 315–342, 1998, doi: 10.1002/(SICI)1096-9845(199804)27:4<315::AID-EQE703>3.0.CO;2-N.
- [28] D. C. Rai and D. R. Sahoo, "Performance-Based Design for Seismic Strengthening of RC Frames Using Steel Caging and Aluminum Shear Yielding Dampers," 2008, [Online]. Available: http://www.iitk.ac.in/nicee/wcee/article/14_09-01-0160.PDF.
- [29] D. C. Rai, P. K. Annam, and T. Pradhan, "Seismic testing of steel braced frames with aluminum shear yielding dampers," *Eng. Struct.*, vol. 46, pp. 737–747, 2013.
- [30] D. R. Sahoo and D. C. Rai, "Seismic strengthening of non-ductile reinforced concrete frames using aluminum shear links as energy-dissipation devices," *Eng. Struct.*, vol. 32, no. 11, pp. 3548–3557, 2010, doi: 10.1016/j.engstruct.2010.07.023.
- [31] L. DiSarno, A. S. Elnashai, and D. A. Nethercot, "Seismic response of stainless steel braced frames," *J. Constr. Steel Res.*, vol. 64, no. 7–8, pp. 914–925, 2008.
- [32] S. El-Khoriby, A. Seleemah, and A. El-Gammal, "Cyclic Performance of Vertical Shear Links Made of Different Metallic Alloys," in *International Conference of Advances in Structural and Geotechnical Engineering*, 2019, p. 14.
- [33] M. D. Engelhardt and E. P. Popov, "Experimental performance of long links in eccentrically braced frames," *J. Struct. Eng.*, vol. 118, no. 11, pp. 3067–3088, 1992.
- [34] C. W. Roeder and E. P. Popov, "Inelastic behavior of eccentrically braced steel frames under cyclic loadings," *NASA STI/Recon Tech. Rep. N*, vol. 78, 1977.
- [35] J. M. Ricles and E. P. Popov, *Dynamic analysis of seismically resistant eccentrically braced frames*. University of California, Earthquake Engineering Research Center, 1987.
- [36] K. Kasai and E. P. Popov, "General behavior of WF steel shear link beams," *J. Struct. Eng.*, vol. 112, no. 2, pp. 362–382, 1986.
- [37] M. G. Vetr, "Seismic behavior, analysis and design of eccentrically braced frames with vertical shear links." University Tech, Darmstadt W. Germany, 1998.
- [38] M. A. Shayanfar, M. A. Barkhordari, and A. R. Rezaeian, "Experimental study of cyclic behavior of composite vertical shear link in eccentrically braced frames," *Steel Compos. Struct.*, vol. 12, no. 1, pp. 13–29, 2012, doi: 10.12989/scs.2012.12.1.013.
- [39] American Institute of Steel Construction, *Seismic Provisions for Structural Steel Buildings: AISC 341-10*, no. 1. Chicago, 2010.
- [40] EN 1998-1, *Eurocode 8: Design provisions for earthquake resistance - Part 1: General rules, seismic actions and rules for buildings*. London: British Standards Institution, 2004.
- [41] I. ANSYS, "ANSYS Workbench Finite Element Analysis Program." Canonsburg, PA., 2020.
- [42] Computers & Structures Inc., "ETABS." Integrated finite element analysis and design of structures, Berkeley, CA, USA, 2018.
- [43] H.-H. Lee, *Finite element simulations with ANSYS Workbench 18: theory, applications, case studies*. SDC publications, 2018.
- [44] M.-R. Shayanfar, A. R. Rezaeian, and S. Taherkhani, "Assessment of the seismic behavior of eccentrically braced frame with double vertical link (DV-EBF)," in *World Conference on Earthquake Engineering*, 2008, vol. 14.
- [45] M. R. Baradaran, F. Hamzezarghani, M. R. Ghiri, and Z. Mirsanjari, "The Effect of Vertical Shear-Link in Improving the Seismic Performance of Structures with Eccentrically Bracing Systems," *World Acad. Sci. Eng. Technol. Int. J. Civil, Environ. Struct. Constr. Archit. Eng.*, vol. 9, no. 8, pp. 1078–1082, 2015.
- [46] T. M. Inc., "MATLAB." The Mathworks Inc., 2013.

-
- [47] OriginLab Corporation, "Origin(Pro)." Northampton, MA, USA, 2019.
- [48] A. S. of C. Engineers, *Seismic evaluation and retrofit of existing buildings: ASCE 41-17*. Reston, Virginia, 2017.
- [49] Y. X. Wen, "Method for random vibration of hysteretic systems," *J. Eng. Mech. Div.*, vol. 102, no. 2, pp. 249–263, 1976.
- [50] C. Durucan and M. Dicleli, "Analytical study on seismic retrofitting of reinforced concrete buildings using steel braces with shear link," *Eng. Struct.*, vol. 32, no. 10, pp. 2995–3010, 2010.
- [51] S. U. Maniyar and D. K. Paul, "Enhancement of Seismic Performance Using Shear Link Braces in a Building Designed Only for Gravity Loads," *J. Inst. Eng. Ser. A*, vol. 93, no. 1, pp. 27–43, 2012.
- [52] Building Seismic Safety Council, *Prestandard and Commentary for the Seismic Rehabilitation of Buildings: FEMA 356*, no. 1. Washington, D.C.: Federal Emergency Management Agency, 2000.